VII. TUBE RESEARCH AND DEVELOPMENT

A. MAGNETRON DEVELOPMENT

Prof. S. T. Martin	V. Mayper
D. L. Eckhardt	R. R. Moats
J. G. Lawton	R. J. Renfrow

1. High-Power 10.7-Cm Magnetron

a. Testing and design

The ceramic-insulated cathode leads have been subjected to cyclic heating to a maximum temperature in excess of 700°C. Two such tests have been made, the metal-ceramic seal failing on the first lead, while a copper-molybdenum soldered joint failed on the second lead after six cycles. The design of the cathode lead has been changed to eliminate this joint.

Some experiments have been performed with butt-type metal-ceramic seals with inconsistent results. On the unsuccessful seals, the ceramic broke apart about 1/16 in. above the metal-ceramic soldered joint. Most of these seals either were broken when removed from the vacuum furnace or broke shortly afterwards even under gentle treatment. The successful seals of the same type and made by the same process were vacuum-tight and withstood much rougher treatment than they would undergo in normal use. Calculations of the stresses in the ceramic have been made and the deductions based on this information are being used in future metal-ceramic seals.

The fact that the power output of our successful high-power magnetrons has apparently been limited by arcing in the pressurized testing tank has led to an investigation of its possible causes. An examination of the ceramic window on MF-6, our last operating tube, showed considerable evidence of arcing across the face of the ceramic. As a result the question of the design of ceramic windows is being investigated more closely. The design criteria and method of assembly of a more satisfactory window have been determined. The new type window will be made in the near future and then subjected to hydraulic pressure in a destruction test.

b. Thoria cathodes

It is tentatively planned to use sheet tantalum end-mounts for the large thoria cathode to be used in the high-power magnetron. A mathematical investigation is being carried out to determine the heat conduction properties of the end-mounts. When the results of this investigation are available, a large thoria cathode will be mounted in a test diode before one is mounted in a magnetron.

c. Auxiliary equipment

The 3500-gauss electro-magnet to be used with the high-power magnetron has been completed, installed and calibrated.

Construction of the high-temperature vacuum furnace has been halted at least temporarily pending the results of an experiment on platinum-brazing the tantalum end-mounts to a thoria cathode in a helium atmosphere. The necessary equipment is now being assembled.

2. Magnetron Research

a. Mode interaction in magnetrons

Further work has been done toward the experimental investigation of the electron stream of a magnetron considered as a simple non-linear circuit element. The work of Van der Pol which considers a non-linear triode oscillator with two degrees of freedom (i.e. two modes) shows that the presence of large-amplitude oscillation in one mode tends to damp other modes. Experimental work has been directed toward the investigation of the effect of large-amplitude π-mode (10.9 cm) oscillation in the 718EY magnetron upon the loaded Q of the $n = 3$ mode (9.5 cm) as measured with an externally supplied signal. The external signal comes from a QK61 magnetron pulsed in synchronism with the 718EY, and the signal is injected into the output circuit of the 718EY as shown in Fig. VII-1.

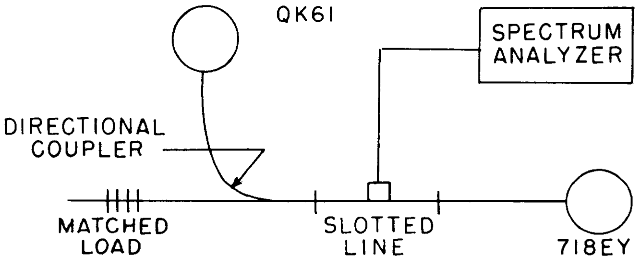

Fig. VII-1 R-F circuit for mode-interaction test.

The first attempt to "cold-test" the $n = 3$ mode with the tube oscillating in the π-mode failed because of the output of considerable energy at 9.5 cm by the 718EY. The energy from this magnetron was much greater than that portion of the QK61 output which reached the spectrum analyzer. Subsequent investigation showed that the latter energy output appeared only at the beginning of the pulse and was of very short duration. This energy apparently resulted from oscillation in the $\gamma = 5$, $n = 3$ mode (where γ is the number of "spokes" in the electron stream). The problem of suppressing the undesired energy coming from the 718EY has been attacked by supplying the signal from the slotted line to the spectrum analyzer through a klystron amplifier (410-R) and pulsing both the QK61 and the klystron in parallel so that this pulse falls entirely within the time of large-amplitude oscillation in the π-mode of the 718EY.

b. Noise properties of the pre-oscillating magnetron

Most of the d-c measurements on an insulated-end-cap tube with an oxide cathode have been completed. These show that for end-ring voltages of 30 percent or more of the anode voltage, the end-ring current is only slightly dependent upon end-ring voltage. However, for lower values of end-ring voltage, end-ring current varies approximately exponentially with the voltage. If the end-rings are considered Langmuir probes, the electron temperature measured in this way is about 50,000°K for an anode voltage of 100 volts, and increases with magnetic field. Presumably the temperature would also increase with anode voltage, but this point has not yet been investigated.

A few measurements of the effect of cathode temperature on the anode current (with end-rings at anode potential) show that for a given anode voltage and magnetic field, the anode current increases slightly as the cathode temperature is decreased until the temperature is so low that the saturation emission is comparable to the anode current. At this point the anode current drops off sharply.

The d-c cutoff characteristics of the tube have been determined at several anode voltages with the end-rings at anode potential. The typical curve of anode current vs. magnetic field (I_a vs. B) is fairly flat with increasing magnetic field until B is approximately that value calculated for d-c cutoff with no initial velocity. When this value is reached, the anode current falls rapidly and exponentially with further increase in magnetic field for a short range, then tails off into what appears to be a very slow exponential decrease corresponding to a much greater electron temperature.

It was discovered in the process of setting up the apparatus for measuring the uhf noise output of the tube that a considerable amount of low frequency noise was developed in the vicinity of 30 Mc for sharply defined values of magnetic field and anode voltage. The values of B and V for this noise peak were plotted (Fig. VII-2) for noise frequencies of 15, 27.5 and 46.0 Mc and in each case gave a straight line. The results can be expressed by the relation

$$B_{(\text{gauss})} = 110 + \frac{360 \times V_{(\text{volts})}}{f_{(\text{Mc})}} \; .$$

This noise peak can be shown to correspond to an electron revolving between 1.5 and 2 times around the cathode for each cycle of r-f output (neglecting the additive constant 110). No adequate explanation of the mechanism by which this noise peak is generated has yet been proposed, but this phenomenon will be investigated.

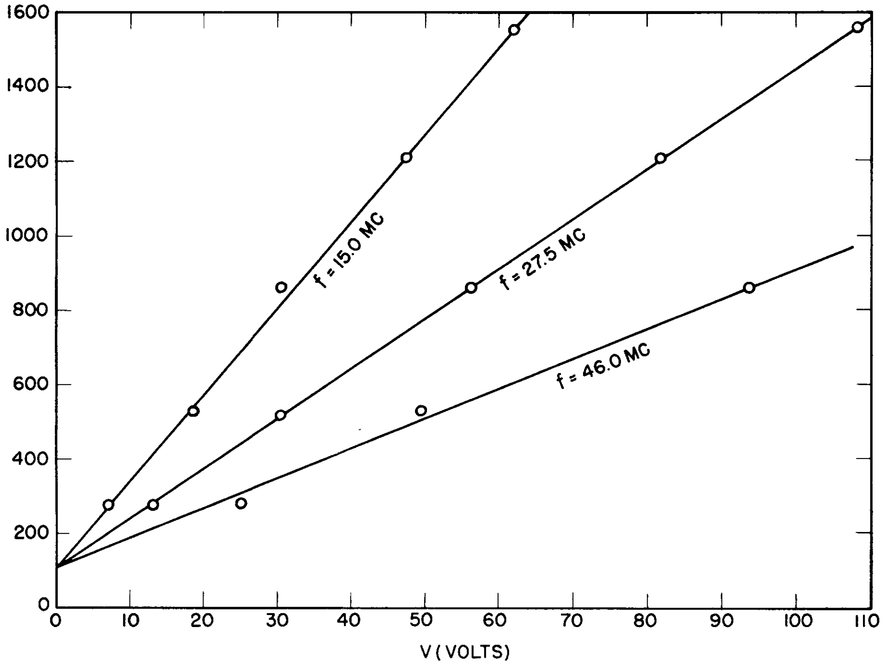

Fig. VII–2 Magnetic field vs. anode voltage for constant frequency of low frequency noise peak.

Before measurements could be completed, there was a mechanical failure of the oxide-cathode insulated-end-cap tube. A new tube is being constructed using a tantalum cathode so that the saturation emission can be more definitely controlled. A preliminary diode has been constructed to determine the operating characteristics of the cathode and the necessary construction techniques. Results show that the cathode will be operated at a temperature of 1800°C. At this temperature the saturation current is in excess of 100 ma.

3. Cathode Research

Two experimental tubes of the type described in the Progress Report, October 15, 1949, have been constructed and processed. The processing of the two tubes was substantially the same except that the first tube was processed for a considerable length of time at 900°C followed by an 8-minute flash to 1000°C while the second tube was processed for about the same length of time but at a maximum temperature of 850°C and a 16-minute flash to 890°C. Emission current was not drawn from either tube until the heating process had been completed and the tube sealed off from the vacuum system.

Contrary to expectations, there was evidence of some cathode activation when d-c emission current was drawn from the cathode. The measured emission deviated considerably from the calculated space-charge emission, and in addition was extremely temperature-sensitive. The emission characteristics of the second tube are shown in Fig. VII-3. At present no explanation is known to explain the departure from the calculated space-charge line and the apparent temperature sensitivity.

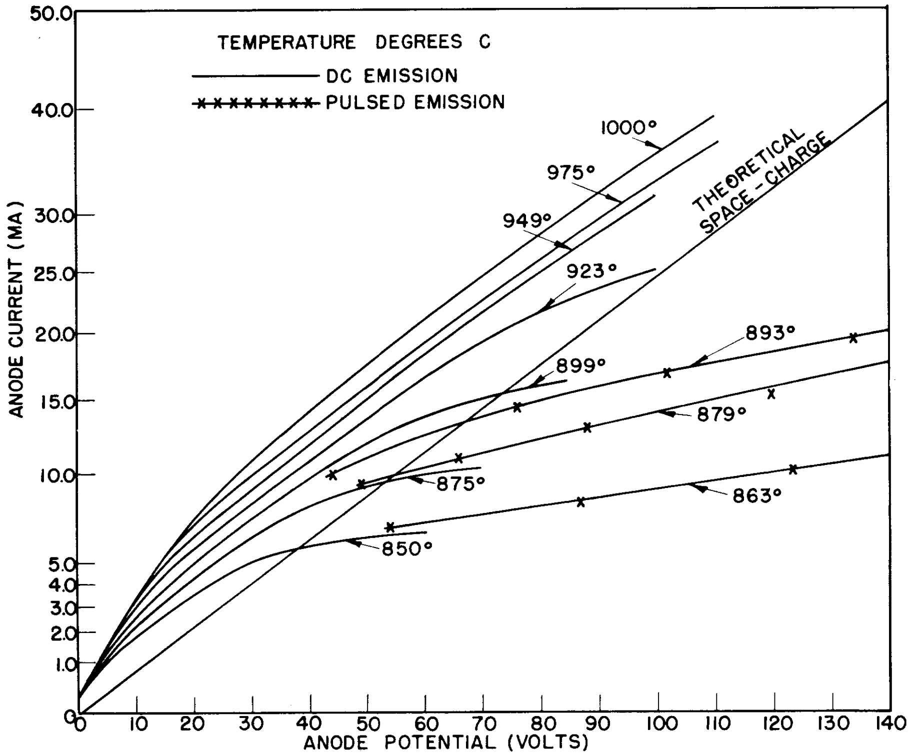

Fig. VII-3
Cathode emission, diode No. 4.

B. TRAVELING-WAVE TUBES

L. D. Smullin L. A. Harris
Prof. L. J. Chu A. Karp
G. W. Zeoli

1. Theoretical Noise Figure of Traveling-Wave Tubes

At the I.R.E. Electronics Conference in June, J. R. Pierce indicated a method of deriving the noise figure of a traveling-wave tube based on the electronic equations of Llewellyn and Peterson (1)(2)(3). We have carried out this analysis with the following general results.

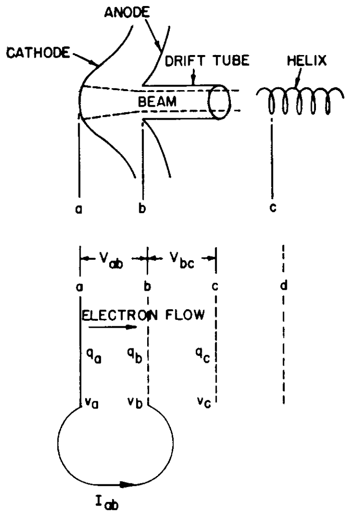

Fig. VII-4 Equivalent diode representation of input end of traveling-wave tube.

The traveling-wave tube is represented by a series of infinite parallel plane diodes as shown in Fig. VII-4. It is assumed that the r-f impedance between anode and cathode, and of the drift tube is zero. Then, on the assumption that the cathode is space-charge limited and that the thermal fluctuation of velocities has a single instantaneous value in each transverse plane, the noise convection current and fluctuation velocity at the input to the helix are

$$i_c = j\, v_a \frac{I_o \omega}{u_o^2} (3d_b - d_c)\, e^{-j(\theta_b + \theta_c)}$$

$$v_c = -v_a \left(\frac{2d_c}{3d_b} + 1\right) e^{-j(\theta_b + \theta_c)}$$

where $\eta = e/m$, t_b = cathode-anode transit time, t_c = drift tube transit time, $\theta_b = \omega t_b >> 1$, $\theta_c = \omega t_c >> 1$, d_b and d_c are the corresponding spacing, and v_a is the velocity fluctuation at the cathode, which according to Rack (4) is given by

$$\overline{v_a^2} = \frac{\eta k T_c B}{I_o} (4 - \pi)$$

where T_c is the cathode temperature, B is the bandwidth, and I_o is the d-c current.

The amplitude E_1 of the growing wave on a helix excited by a current-and velocity-modulated beam is

$$E_1 = \frac{\beta_o\, C \left[\frac{2V_o Ci}{jI_o}\left(\frac{1}{2} - j\frac{\sqrt{3}}{2}\right) - \frac{2V_o}{u_o}\, v\left(\frac{\sqrt{3}}{2} - \frac{j}{2}\right)\right]}{3\left(\frac{1}{2} + j\frac{\sqrt{3}}{2}\right)}$$

where C is the usual gain parameter, $\beta_o = \omega/u_o$, $u_o = \sqrt{2\eta V_o}$. Putting in the expressions for i and v,

$$\left|E_{1_n}\right|^2 = \frac{4\beta_o^2 C^2 V_o^2 (2\alpha + 1)^2\, \overline{v_a^2}}{9u_o^2}\left(X^2 - X\sqrt{3} + 1\right)$$

where $X = -r\omega C\sqrt{\frac{2\pi\epsilon u_o}{\eta I_o}}\left(\frac{1-\alpha}{2\alpha+1}\right)$, $\alpha = \frac{d_c}{3d_b}$, and r = the cathode radius. The noise figure is given by

$$F = \frac{\left|E_{1_n}\right|^2 + \left|E_{1_T}\right|^2}{\left|E_{1_T}\right|^2} \simeq \frac{\left|E_{1_n}\right|^2}{\left|E_{1_T}\right|^2}$$

where $\left|E_{1_T}\right|^2$ is the noise power due to the antenna resistance. Then

$$F = \frac{(2\alpha + 1)^2\, I_o\, \overline{v_a^2}\left(X^2 - X\sqrt{3} + 1\right)}{4\eta CkTB}$$

and putting in the value of $\overline{v_a^2}$

$$F = \frac{0.214\; T_c (2\alpha + 1)^2}{CT}\left(X^2 - X\sqrt{3} + 1\right) \quad .$$

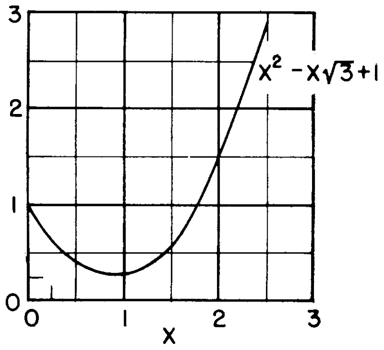

Fig. VII-5

The quantity $(X^2 + 1 - X\sqrt{3})$ is plotted in the accompanying figure and it is seen to have a rather broad minimum. Thus, to a good approximation

$$F \propto \frac{(2\alpha + 1)^2}{C}$$

which indicates the extreme importance of reducing the drift tube length between the gun anode and the beginning of the uniform section of the helix.

a. Experimental work

Since this theoretical analysis was completed, the experimental effort has been directed towards the design of a 3-cm, 1000-volt, 1-ma tube to have a $C \simeq 0.015$. The most serious difficulty has been in finding a design with $d_c < 3d_b$ $\left[(2\alpha + 1)^2 < 9\right]$. For reasonable values of X, and with $T_c = 1000°K$,

$$F \simeq \frac{0.28(2\alpha + 1)^2}{C}$$

so for $C = 0.015$, and $d_c = 6d_b$, $F \simeq 25$ db.

L. D. Smullin

References

(1) F. B. Llewellyn, "Electron Inertia Effects", Cambridge University Press (1939).

(2) F. B. Llewellyn and L. C. Peterson, Proc. I.R.E. 32, 144 (1944).

(3) L. C. Peterson, Proc. I.R.E. 35, 1264 (1947).

(4) A. J. Rack, B.S.T.J. 17, 592 (1938).

2. Microwave Noise Studies

The last quarter has been spent in building a noise tube consisting of a 2000-volt, 5-ma Pierce gun, and a 10-cm resonant cavity; a variable Q filter cavity to put in front of our standard noise source to restrict its bandwidth to that of the test tube; and various other bits of r-f circuitry.

A. Karp

3. Dense Electron Beams in Axial Magnetic Fields

Progress during the last quarter has been confined to theoretical work on this problem.

The basic assumptions on which the entire analysis rests are axial symmetry and radial non-crossing of electrons. By this we mean that electrons travel in cylindrical shells which may pulsate in radius but never pass through each other. The principal justification for this assumption is mathematical convenience. It enables us to write the scalar electric potential ϕ as seen by any electron in the form

$$\phi = \alpha \ln \frac{r}{r_0} + \gamma$$

where r is the distance of the electron from the axis and r_o is the value of r at which the electron experiences no radial force. The values of α and γ defined by this equation are determined from a solution for the average potential, assuming the beam to be uniform along its length and subject to the boundary conditions imposed by inner and outer electrodes where they are present.

The average charge distribution in the beam is taken as a function of radius only

$$\rho = \sum_{n=0}^{\infty} \rho_n r^n \quad \text{for} \quad r_a \leqslant r \leqslant r_b$$

$$\rho = 0 \quad \text{for} \quad \begin{cases} r < r_a \\ r > r_b \end{cases}$$

where the series need be taken over positive powers only without loss in generality.

The condition that the electron experience no radial force at r_o is met if the following equation is satisfied

$$\Psi_c = \Psi\sqrt{1 + K\alpha}$$

where $K = \frac{e}{m}/\omega_H^2 r_o^2$; $\omega_H = \frac{e}{m}\frac{B}{2}$; $\Psi = \pi r_o^2 B$, the flux linking the circle of radius r_o; and Ψ_c = the flux linking a circle at the cathode drawn through the starting position of the electron in question. It is shown by a variational method that any charge distribution is a possible equilibrium configuration so long as the proper relation between Ψ and Ψ_c is maintained. If the functional form of $\Psi_c(r_o)$ is limited by other considerations, as it generally is, this constitutes a limitation on the types of charge distribution physically attainable.

If we use the conditions and equations outlined above, the equations of motion are easily formulated. Substituting $R = r^2$ and neglecting all powers above the first in the expansion for the logarithm lead to a linear differential equation in R. Its solution is

$$\frac{R}{R_o} = 1 + \Delta + \sqrt{(2\Delta)} \sin ct$$

where $\Delta = \dfrac{K(\gamma - V) + \sqrt{1 + K\alpha}}{1 + \frac{K\alpha}{2}} - 1$, $c = -2\omega_H\sqrt{1 + \frac{K\alpha}{2}}$, $R_o = r_o^2$, and V = the voltage corresponding to the axial velocity, $\dot{z}^2 = -2\,\frac{e}{m}\,V$.

This solution which is valid for small radial oscillations holds for both hollow and solid beams. The only differences between these two cases are in the functional forms of α and γ. It is to be noted that in only one special case is the solution completely consistent with the assumption of non-crossing which requires that the frequencies and phases of oscillation be the same for all electrons. This is true only in the case of a solid beam, or of a hollow beam with a uniform charge distribution and the appropriate inner and outer electrode voltages. The usefulness of all the other solutions is a matter to be settled by experiment.

If we go on the supposition that all solutions will be useful in practice, we can set up a chart useful in the design of electron beam and magnetic field systems. To do this we set $\Delta = 0$ and plot a surface defined by this equation. The axes are α and γ plotted linearly and $|K|$ plotted logarithmically. The specifications of the type of beam desired serve to define the differences between α's, and γ's, and the ratio between $|K|$'s for any pair of electron shells in the beam. These differences define three sides of a rectangular prism and the design procedure consists of fitting the end points of a diagonal of the prism into the surface, of course maintaining the orientation of the prism. The proper parameters are then determined from the position of the diagonal in the surface. This procedure is more conveniently carried out by moving a triangle over a family of curves. The chart is useful in evaluating the amplitude of oscillation that results if the exact design conditions cannot be met because of other restrictions.

The theory indicates that it is possible to have a stable hollow beam with no magnetic field along the greater part of its length. This is possible only with a hollow beam because a radial electric field tending to pull electrons toward the axis is necessary. The flux Ψ_c through the cathode is also a necessary part of the scheme but the flux Ψ elsewhere can be eliminated. It would appear that this case may be of considerable practical significance.

The criticalness of thermal velocities mentioned in the last report is not correct. Thermal velocities may have considerable influence on the beam if any magnetic flux is allowed to penetrate the emitting surface obliquely. The magnetic field must be normal to the cathode in regions of low electron velocity.

L. A. Harris

C. THE GENERATION OF MILLIMETER AND INFRA-RED RADIATION BY ACCELERATED ELECTRONS

P. D. Coleman

In the Progress Report, April 15, 1949 it was pointed out that the principal problem in designing a generator based on the radiation from accelerated electrons was to obtain coherence. In practice this means building a 1-2 Mev, 0.2-0.3 ampere peak, very short pulsed electron source.

The generator under development is a microwave cavity powered by two HK7 magnetrons. Electrons are injected into the cavity from a sharply focused Pierce electron gun, the electron beam being modulated by a bunching cavity (Fig. VII-6). Initially a Sperry XZF8529 klystron was tried as an electron source, but in spite of considerable modification, this tube proved unsatisfactory for the purpose intended.

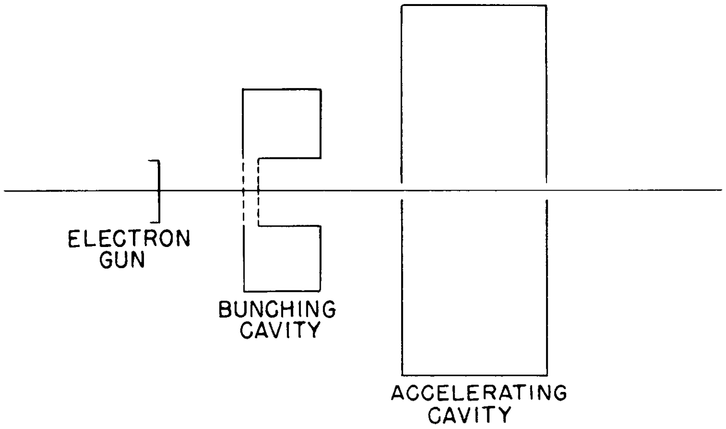

Fig. VII-6 Schematic diagram of cavity accelerator.

The development of a 20-kv pulsed gun and bunching cavity has been under way. By designing the electron gun, and the bunching and accelerating cavities as a unit, it is theoretically possible to obtain electron space bunching of the order of 0.1 mm with 10^8 electrons per bunch.

One tube has been built and tested; two more are under construction. At the moment, the problem has been the Pierce gun, in that it has been difficult to spin the tantalum electrodes to the exact shape as determined by an electrolytic tank.

The linear accelerator group has been interested in this pulse accelerator. Recently they have begun a model based on the above design to investigate if it could be used for electron injection into the main linear accelerator.

* * *